AGU PUBLICATIONS

JGR

Journal of Geophysical Research: Space Physics

RESEARCH ARTICLE
10.1002/2014JA020912

Key Points:
- Transpolar arc was observed twice after the entry events
- High-latitude MR may explain its day part
- There are some indications of two-part structure of the arc

Supporting Information:
- Movie S1

Correspondence to:
Q. Q. Shi and B. Mailyan,
sqq@sdu.edu.cn;
bagrat_mailyan@yerphi.am

Citation:
Mailyan, B., et al. (2015), Transpolar arc observation after solar wind entry into the high-latitude magnetosphere, *J. Geophys. Res. Space Physics*, *120*, 3525–3534, doi:10.1002/2014JA020912.

Received 8 DEC 2014
Accepted 26 MAR 2015
Accepted article online 31 MAR 2015
Published online 13 MAY 2015

Transpolar arc observation after solar wind entry into the high-latitude magnetosphere

B. Mailyan[1,2], Q. Q. Shi[1], A. Kullen[3], R. Maggiolo[4], Y. Zhang[5], R. C. Fear[6], Q.-G. Zong[7], S. Y. Fu[7], X. C. Gou[1], X. Cao[8], Z. H. Yao[9], W. J. Sun[7], Y. Wei[8], and Z. Y. Pu[7]

[1]School of Space Science and Physics, Shandong University, Weihai, China, [2]Cosmic Ray Division, Yerevan Physics Institute, Yerevan, Armenia, [3]Space and Plasma Physics, School of Electrical Engineering, Royal Institute of Technology, Stockholm, Sweden, [4]Belgian Institute of Space Aeronomy, Space Plasma, Brussels, Belgium, [5]Applied Physics Laboratory, The Johns Hopkins University, Laurel, Maryland, USA, [6]School of Physics and Astronomy, University of Southampton, Southampton, UK, [7]Institute of Space Physics and Applied Technology, Peking University, Beijing, China, [8]Institute of Geology and Geophysics, Chinese Academy of Sciences, Beijing, China, [9]Mullard Space Science Laboratory, University College London, London, UK

Abstract Recently, Cluster observations have revealed the presence of new regions of solar wind plasma entry at the high-latitude magnetospheric lobes tailward of the cusp region, mostly during periods of northward interplanetary magnetic field. In this study, observations from the Global Ultraviolet Imager (GUVI) experiment on board the TIMED spacecraft and Wideband Imaging Camera imager on board the IMAGE satellite are used to investigate a possible link between solar wind entry and the formation of transpolar arcs in the polar cap. We focus on a case when transpolar arc formation was observed twice right after the two solar wind entry events were detected by the Cluster spacecraft. In addition, GUVI and IMAGE observations show a simultaneous occurrence of auroral activity at low and high latitudes after the second entry event, possibly indicating a two-part structure of the continuous band of the transpolar arc.

1. Introduction

During periods of northward interplanetary magnetic field (IMF), geomagnetic activity is generally quiet, but solar wind plasma can penetrate and be stored in the magnetosphere. Recently, a new region of solar wind plasma entry into the terrestrial magnetosphere, in the lobes tailward of the cusp, was reported, and high-latitude magnetic reconnection was suggested to be the most probable mechanism of the entry [*Shi et al.*, 2013]. Higher-energy ions have been found by *Fear et al.* [2014] and interpreted as due to magnetotail reconnection during periods of northward IMF. Since these events are rare, the fate of the entered plasma has not been widely studied. It is not known whether those plasma entries will contribute to aurora. *Huang et al.* [1989] and *Fear et al.* [2014] have reported that the higher-energy ions in the lobe are associated with transpolar arcs, which are a fascinating phenomenon appearing occasionally during northward IMF. Transpolar arcs are aurora structures extending poleward the auroral oval.

The transpolar arcs extending from the nightside to dayside connecting the oval from both sides are called theta auroras (since they resemble a Greek letter theta). The theta aurora was observed several decades ago in 1982 [*Frank et al.*, 1982, 1986], but its formation mechanism is still poorly understood. For example, a theta aurora associated with magnetotail plasma was reported by *Huang et al.* [1989]. For many years, it was thought that the transpolar arcs form symmetrically in both hemispheres based on several studies [see, for example, *Craven et al.*, 1991]. *Ostgaard et al.* [2003] showed a nonconjugate theta aurora, when the arc was observed only in one hemisphere.

Transpolar arcs can have different shapes, and their location can change with time or be static [e.g., *Mawson* 1916; *Zhu et al.*, 1997; *Kullen*, 2012]. Statistical studies have previously shown that the occurrence of these structures is correlated with high values of solar wind velocity and IMF magnitude [*Kullen et al.*, 2002]. It was reported that IMF B_y value and its variation are controlling the location and the motion of transpolar arcs [*Fear and Milan*, 2012a, and references therein]. The effect of the IMF B_y component is opposite in the northern and southern hemispheres.

While some studies explaining the formation of the transpolar arcs suggest that they lie on closed field lines [e.g., *Frank et al.*, 1986], others require an open field line configuration [*Gussenhoven and Mullen*, 1989]. The

models that are based on the closed field line configuration require reconnection in the magnetotail [*Milan et al.*, 2005] or a large-scale deformation of the magnetotail [e.g., *Frank et al.*, 1986; *Kullen*, 2000]. Reviews of the various transpolar arc models can be found in, e.g., *Zhu et al.* [1997] or *Fear and Milan* [2012a].

Recently, many of the models have been rejected due to their inconsistency with the increasing number of new observations. Nowadays, most models are based on IMF B_y control, like, for example, models suggested by *Kullen* [2000] and *Milan et al.* [2005]. The B_y component of IMF causes a twist in the magnetotail, which consequently causes the formation of transpolar arcs at quiet periods without much substorm activity (either due to magnetotail reconnection in the case of *Milan et al.*'s [2005] mechanism or as a direct result of a change in the twist of the tail according to *Kullen* [2000]). The IMF B_y control of transpolar arc location at its formation as well as a connection to nightside ionospheric flows indicating that magnetotail reconnection have been predicted by *Milan et al.*'s [2005] model are observed and have been reported in statistical studies [*Fear and Milan*, 2012a; *Fear and Milan*, 2012b]. *Milan et al.*'s [2005] model successfully describes many properties of the arcs origin. A case study by *Goudarzi et al.* [2008] showed some consistency with Milan's model. On the other hand, the model by *Kullen* [2000] interprets the appearance and motion of transpolar arcs after an IMF B_y sign change as being the result of a rotation of a twisted magnetotail, which causes a strip of closed field lines to move over the polar cap. Simulation studies by *Naehr and Toffolletto* [2004] suggest that the arc will not extend to the dayside if only a tail deformation is responsible for the occurrence of a transpolar arc. Other simulations of an IMF B_y sign change showed similar results. While a strip of closed field lines moving over the polar cap was produced in all reported simulations, it does not stretch completely to the dayside [e.g., *Slinker et al.*, 2001; *Kullen and Janhunen*, 2004]. Consequently, some other mechanism must be involved to explain the origin of a transpolar arc. Almost all of the previous models propose that the transpolar arc develops from one source, either from the dayside or from the nightside [*Chiu et al.*, 1985; *Lyons*, 1985; *Reiff and Burch*, 1985; *Makita et al.*, 1991; *Sojka et al.*, 1994; *Newell and Meng*, 1995; *Rezhenov*, 1995; *Chang et al.*, 1998; *Kullen*, 2000; *Milan et al.*, 2005]. *Eriksson et al.* [2005] proposed that the different parts of a transpolar arc may be created by two different mechanisms at the dayside and nightside parts of the aurora oval, respectively. They suggest that the dayside part can be driven by high-latitude reconnection and the nightside part can be related to the pressure gradient-driven generation of upward field aligned currents [*Vasyliunas*, 1970] of the Harang discontinuity [*Erickson et al.*, 1991]. In *Eriksson et al.* [2005], two different plasma flow directions on the same transpolar arc can be seen; however, they do not show any evidence for the proposed generation mechanisms. They suggest that these two processes maybe often couple together and result in one apparently continuous transpolar arc. However, in a recent case study by *Fear et al.* [2014], a transpolar arc formation was observed with a hot plasma source, similar to that in the plasma sheet. The hot plasma electron pitch angle distribution peaked perpendicular to magnetic field direction, which is a strong evidence that the plasma along the transpolar arc was on closed field lines. These observations were argued to be consistent with those predicted by *Milan et al.* [2005].

Shi et al. [2013] have discussed several possibilities for their plasma observations, which they called "entry events," and proposed that they were most probably caused by high-latitude reconnection. We do not totally rule out other possibilities such as tail reconnection suggested by *Fear et al.* [2014]. However, throughout this paper, we use the term "solar wind entry event" or "entry event" to refer to plasma signatures of the type observed by *Shi et al.* [2013], and studying the details of the entry event formation is beyond the scope of this paper.

In this work, based on multi-instrument observations, we present a case showing the formation of the transpolar arc in the south hemisphere after two solar wind plasma entry events. We also show some indication that a transpolar arc can originate both from the dayside and nightside at the same time.

2. Data Sources

To investigate the link between transpolar arcs and solar wind entry events, data from several spacecraft missions were used. First, the event was identified by the Global Ultraviolet Imager (GUVI) instrument on board the TIMED mission. Its low circular orbit at an altitude of 630 km results in images at a very high spatial resolution, reaching 7 km resolution at nadir [*Paxton et al.*, 2004] for various wavelengths from 121.6 nm up to 180.0 nm. However, the spatial coverage of GUVI is limited. The full view of the aurora oval

and polar region at higher time resolution of the transpolar arc is provided by the IMAGE/FUV instrument [*Mende et al.*, 2000] with spatial resolution 60 km. Data from the Wideband Imaging Camera (WIC) are used with 2 min cadence at 140–180 nm wavelengths.

The low-altitude orbit (840 km) Defense Meteorological Satellite Program (DMSP) satellites carrying plasma instruments allow for measurement of electron and ions precipitation in the energy range from several tens of ev to keV energy range [*Hardy et al.*, 2008]. Data from the DMSP f-13 are analyzed in this work.

For solar wind entry plasma parameters, observations of Cluster ion spectrometer (CIS) experiment [*Reme et al.*, 2001] and fluxgate magnetometer (FGM) experiment [*Balogh et al.*, 2001] are used.

ACE spacecraft data are used for the IMF [*Smith et al.*, 1998] and plasma measurements of the solar wind [*McComas et al.*, 1998].

3. Transpolar Arc on 20040927

The criteria of the solar wind entry event selection are reported in the paper by *Shi et al.* [2013]. To ensure that the Cluster is in the lobe, the ratio of plasma to magnetic pressure, i.e., the plasma beta, was required to be less than 0.05, and the ion density should be lower than 1 cm^{-3}. In addition, the ion energy should be centered between 0.7 and 2 keV to confirm the solar wind origin of the plasma and to exclude for instance upflowing ionospheric ions. A more detailed description of the solar wind entry event selection criteria can be found in *Shi et al.* [2013]. Using these criteria, a total number of 104 events were found occurring between 2001 and 2004. For these events, *Shi et al.* [2013] found that the ratio of oxygen to proton number density is decreased compared to the ambient regions, indicating that they have a solar wind origin. This ratio will be higher for lobe or ionospheric upflowing ions [see, e.g., *Maggiolo et al.*, 2011]. We should also note that the event studied by *Fear et al.* [2014] was not selected by these criteria because of the relatively higher-energy ions in that event.

Examining the GUVI data during the time periods corresponding to the entry events list of *Shi et al.* [2013], 15 transpolar arcs were identified. One of the most remarkable theta auroras was observed by GUVI on 27 September 2004. During a time period of northward IMF B_z and enhanced negative B_y on this day, two consecutive plasma entries (as indicated by purple boxes in Figure 1) in the high-latitude magnetosphere tailward of the cusp were observed by Cluster. The initial and final positions of Cluster for this event were [−6.088, 4.075, and −11.818] and [−5.062, 3.873, and −11.596] Re in GSM coordinates.

In Figure 1, Cluster data from CIS and Plasma Electron and Current Experiment and IMF data from OMNI are shown along with IMAGE WIC and TIMED/GUVI keogram. Due to the orbit of TIMED and to the scanning mode of GUVI, its keogram looks different since various parts of the aurora map are taken at different times. Furthermore, GUVI cannot observe all magnetic local time (MLT) regions and the entire polar cap. Thus, the GUVI keogram is presented for the time interval ~21:35–21:44 when the spacecraft moves over the 60–90° magnetic latitude (MLAT) region. The intensifications of emissions are detected by GUVI in the polar region at about 21:43–21:44. Since IMAGE/WIC can observe the entire polar cap every 2 min, the keogram is plotted for a 1 h MLT sector centered at 23:00 MLT, where the transpolar arc was observed. The MLAT range from 60 to 90° is shown in the IMAGE keogram. However, above 85°, airglow does not allow observation of the aurora. As we can see, the transpolar arc intensification observed by IMAGE spreads from low latitudes right after the entry event. After the two entry events (right after purple boxes from Figure 1), we can see higher-energy tail ions which can be due to tail reconnection as suggested by *Milan et al.* [2005] and *Fear et al.* [2014]. GUVI observed the auroral activity at high latitudes just at the time of the decrease of the transpolar arc, observed by IMAGE.

At the time of the entry event, Cluster's foot point maps to the region near the South Pole, where the transpolar arc is observed by TIMED/GUVI and IMAGE/WIC instruments. Cluster's foot point coordinates were [−88.2, 10.4] and [−86.7, 12.1] MLAT-MLT, respectively, at the beginning and at the end of the time period of interest, as indicated in Figures 2 and 3.

From top to bottom, (a) Cluster ion spectrogram, (b) ion density measured by Cluster, (c) Cluster electron spectrogram, (d) interplanetary magnetic field in GSM coordinates, (e) keogram of IMAGE/WIC instrument, and (f) TIMED/GUVI keogram are presented. The two purple boxes indicate the solar wind entry events. The vertical orange lines indicate the start of transpolar arc extension and intensification.

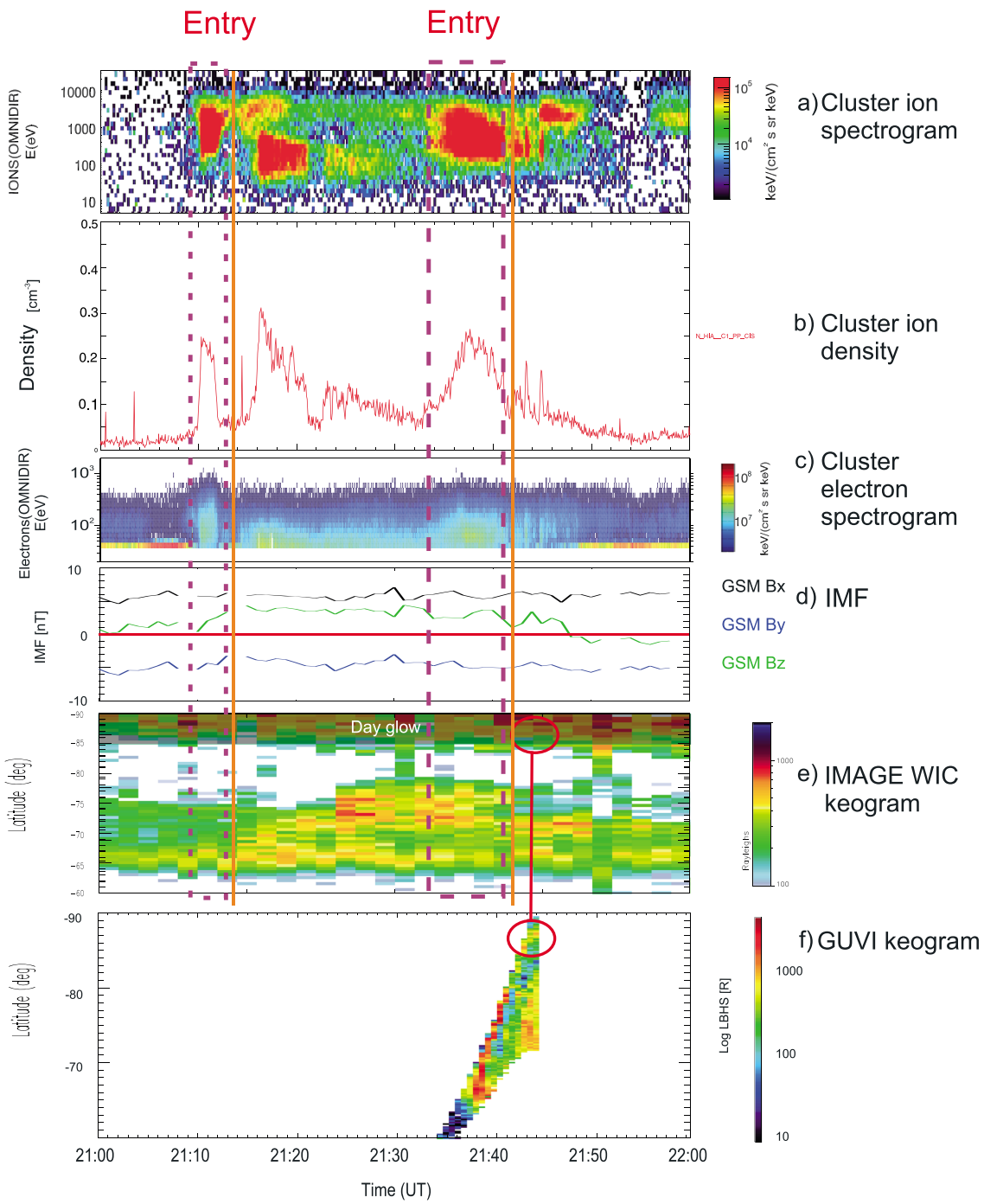

Figure 1. (a–f) Comparison of the entry plasma by Cluster with IMAGE and GUVI keograms.

The red circles are drawn to make easier the comparison between TIMED/GUVI observations at highest latitudes and IMAGE/WIC data at the same time (~21:43 UT). Data from the moment of time, marked by the two circles, show that TIMED/GUVI still observes the arc in a region where at IMAGE/WIC, dayglow dominates.

In order to study the solar wind conditions during the 27 September 2004 event, we checked the ACE IMF and plasma data. To take into account the measurements carried at large distance away from the Earth, a time shift has to be done. The simple "flat delay" method, just dividing the distance between ACE and Cluster to the solar wind average velocity V_x component calculated an hour before the entry

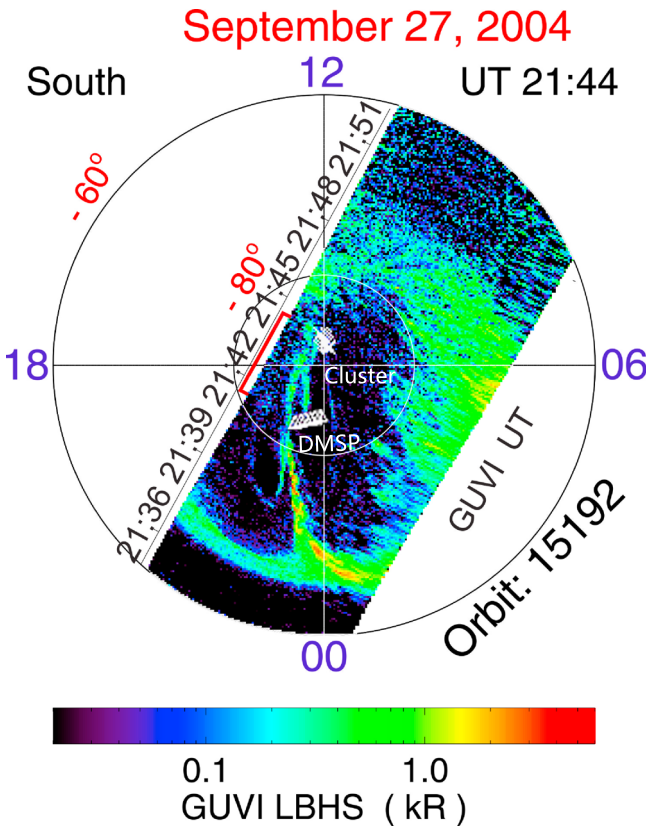

Figure 2. GUVI observations of the transpolar arc: aurora map and time to each pixel axis. The crosses are for Cluster, and the triangles are for DMSP foot points. On the left part of the image, the time period (21:41–21:44) is marked by a red line, when GUVI observes the arc at high latitudes, while IMAGE/WIC observes the decreased intensity of the arc at latitudes between 78 to 84° (at nightside) and dayglow at latitudes higher than 84° (see also Figures 1e and 1f).

[*Mailyan et al.*, 2008], can give good enough results compared with more sophisticated methods. However, we used OMNI data (http://omniweb.gsfc.nasa.gov) with already calculated time shift [*King and Papitashvili*, 2005].

In Figure 1d, the IMF components are shown. At the time when the transpolar arc intensifies, as we can see, the IMF B_z component becomes northward at 21:10 UT. The IMF turns southward again at 21:48 UT, after an increase in the luminosity of the transpolar arc. The arc was found in the dusk in the southern hemisphere when IMF $B_y < 0$, which is consistent with previous observations showing that duskside arcs appear mainly during dawnward IMF in the southern hemisphere and during duskward IMF in the northern hemisphere [e.g., *Elphinstone et al.*, 1995; *Kullen et al.*, 2002, and references therein].

The GUVI aurora map is presented in Figure 2 in Lyman-Birge-Hopfield short filter band 140–150 nm in magnetic local time and latitude frame. Fine structures in the apparent continuous arc can be seen. However, as it was mentioned, each pixel of the aurora map corresponds to different time moments. The corresponding UT times are shown on the inclined axis. As we can see, GUVI observations at the highest latitudes (absolute magnetic latitude $> 80°$) correspond to the times between 21:43 and 21:45. At the time of the highest magnetic latitude at 21:44 UT, we can clearly see structured optical emissions in the South Pole region. At this time, the Cluster foot point mapped to the same region of the observed by GUVI transpolar arc.

The same theta aurora observed also by IMAGE/WIC instrument is shown in Figure 3. Unfortunately, due to the airglow, it is only possible to see the nightside part in WIC data, while the dayside image is available only from GUVI. IMAGE/WIC spatial resolution is much lower in comparison with GUVI; hence, the small branches in the arc cannot be seen by IMAGE. However, the temporal resolution of IMAGE data allows us to see the time evolution of the arcs (Figure 3). At 21:21, we can see an intense aurora activity starting in the midnight region, thereafter a gradual extension of the arc toward the polar region that continues until 21:31 when the transpolar reaches the dayglow region. The transpolar arc becomes considerably weaker at 21:43–21:45, and then a new intensification starts around 21:48. After the second entry event at 21:41–21:44 when we see a weakening arc in the nightside region and cannot observe the dayside because of the dayglow in the WIC image, GUVI observed the arc at the highest latitudes. This time sequence can be clearly seen from the last panels of Figure 1. The red circles show the location where GUVI observed the arc intensification at these latitudes, while the IMAGE data are dominated by airglow. During that time period, the arc luminosity decreases, as is evident from the IMAGE keogram in Figure 1e (the area below the red circle). The similarity of the arc shape at low latitudes is also apparent from the comparison of Figures 2 and 3 IMAGE/WIC aurora map at 21:31 UT. However, WIC data for 21:43 at low latitudes look quite different from GUVI observations at high latitudes.

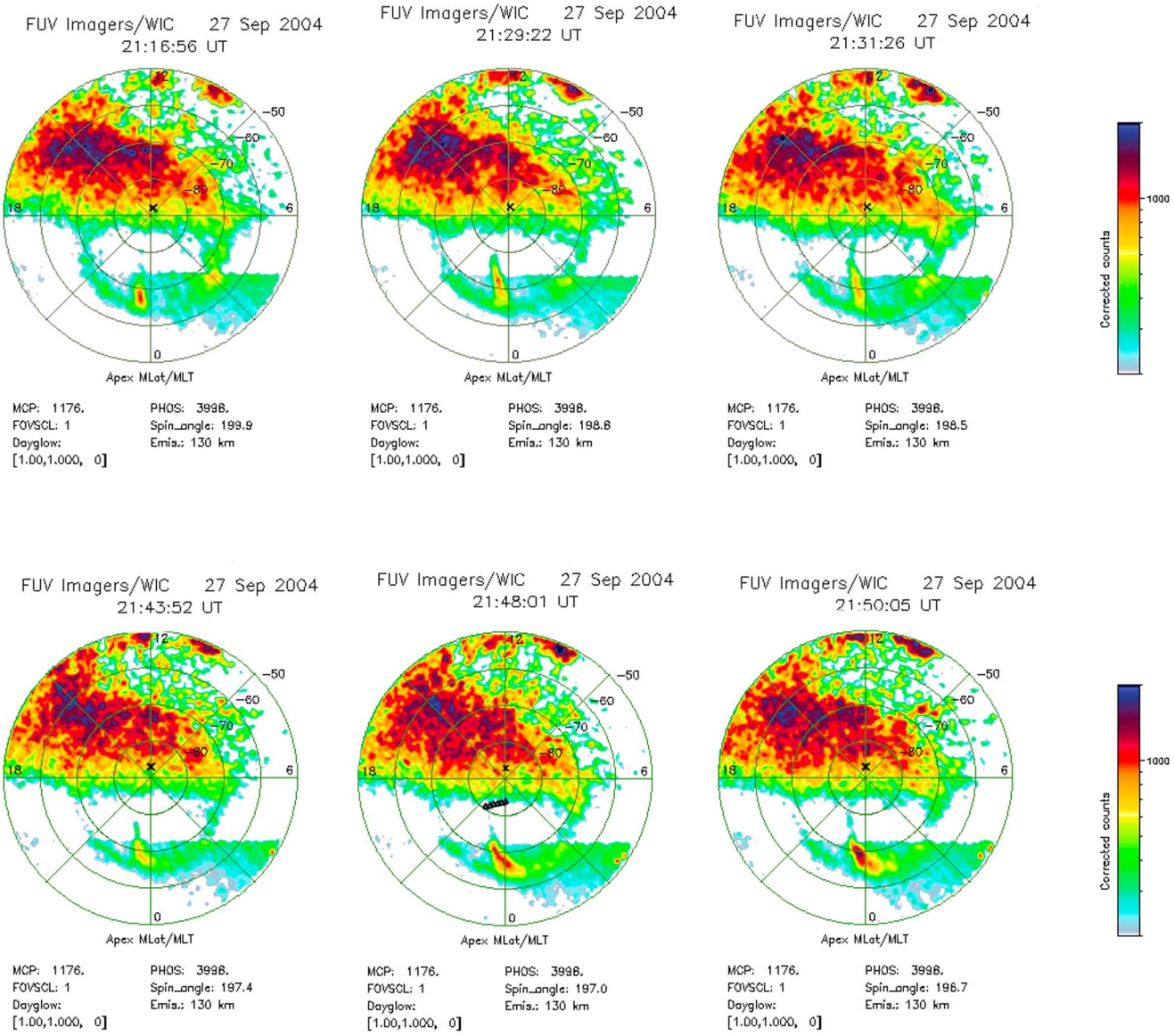

Figure 3. IMAGE WIC observations of the theta aurora. The crosses correspond to the foot points of Cluster between 21:00 and 22:00. The area above the lines connecting 06:00 to 18:00 MLT is dayglow. The straight cut at nightside caused by uncertainties of airglow correction and has no physical meaning.

The DMSP f-13 spacecraft also passed above the transpolar arc when it was observed by GUVI. The transpolar arc as we saw is located at a narrow sector near 23:00 MLT. In Figure 4, we can see electron and ion measurements by DMSP. The red box corresponds to the time when DMSP f-13 is at the region of the interest. In the picture, we can see "inverted-V" structures, characteristic of electrons accelerated downward by the electric field, causing aurora. Two such structures are seen at 21:46–21:47 marked by the box. The average energy of the electrons is about several hundreds eV. The values are in a good agreement with typical values reported in previous studies [see, for example, *Park et al.*, 2012]. Ion precipitations are much weaker than the electron precipitations, which mean that DMSP passes an aurora precipitation region, where electrons move toward the Earth and ions flow in opposite direction [*Iijima et al.*, 1984].

DMSP data of electron precipitation show several inverted-V structures across the entire polar cap. This fits well with several less intense polar cap auroral arcs in the GUVI image. These features agree well with Sun-aligned arcs, which are typical for northward IMF [e.g., *Valladares et al.*, 1994; *Shiokawa et al.*, 1997]. *Kozlovsky et al.* [2007] suggested that they are caused by solar wind entry into the closed magnetosphere.

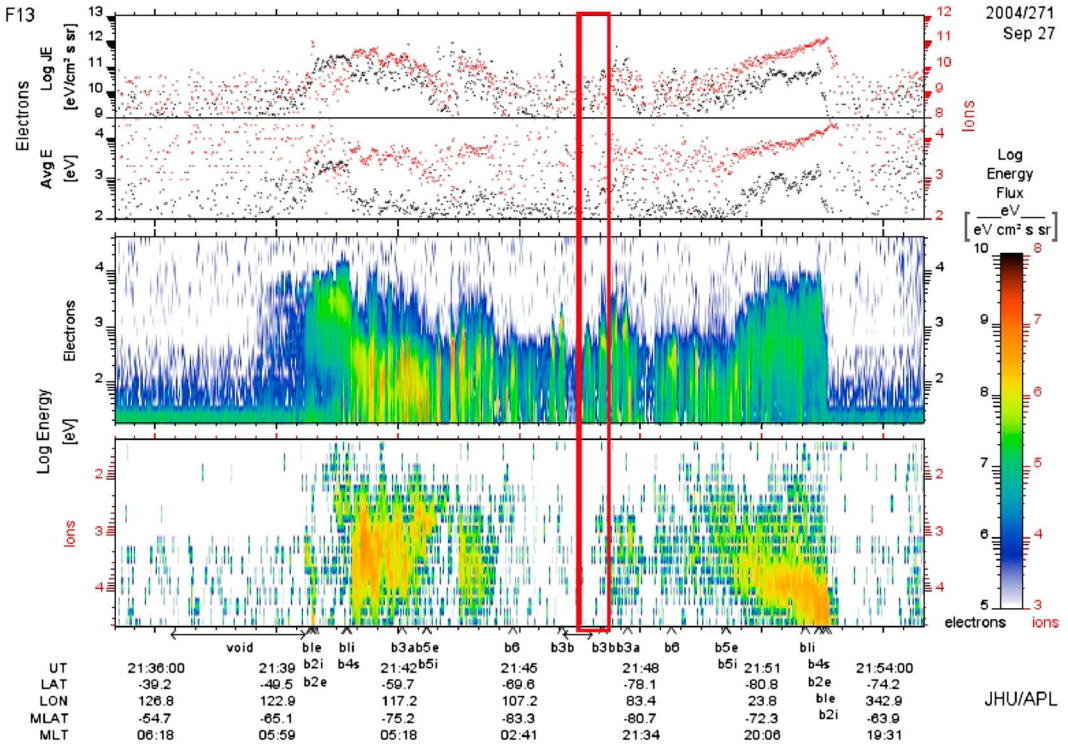

Figure 4. DMSP f-13 observations of precipitating ions and electrons.

4. Discussion and Conclusions

We have presented a transpolar arc observed by two different imagers—the high-altitude orbit IMAGE which gave the global aurora map and time evolution information and the lower-altitude orbit GUVI onboard TIMED which gave more detailed structure of the theta aurora and the information about the dayside polar regions that are not visible on IMAGE due to the dayglow.

It is clear from GUVI images that the arc already existed when the auroral intensification spreads along the arc. This suggests that an intensification occurs of an already existing arc which may have been formed by the mechanism as proposed in *Milan et al.* [2005].

It is known that, e.g., solar wind pressure pulses can brighten up already existing transpolar arcs [*Liou et al.*, 2005]. The duskward position of the transpolar arc on the southern hemisphere and the negative IMF B_y value also are in an agreement with Milan's model as well as consistent with other models as stated above.

On the other hand, Cluster observed solar wind entry events at high latitudes. The Cluster foot point maps to the dayside part of the transpolar arc observed by GUVI. Observations of this particular event show that right after the solar wind entry, a polar cap arc starts to extend from the nightside toward the dayside. On the GUVI image, this transpolar arc seems to consist of two branches (Figure 2).

Ionospheric flows accompanying the formation of transpolar arcs have been reported in several studies. The Super Dual Auroral Radar Network (SuperDARN) array of high-frequency radars [*Baker et al.*, 2007] provides ionospheric convection pattern, which is extremely valuable data for transpolar arc studies [see, for example, *Koustov et al.*, 2008, 2012]. We checked the SuperDARN data (not shown) for the convection pattern in the ionosphere. Flows on the nightside indicate reconnection at the magnetotail. However, the smaller number of the stations in southern hemisphere does not allow an appropriate analysis of the event from the ionosphere convection point of view.

The idea of a two-part structure of transpolar arcs has been proposed by *Eriksson et al.* [2005]. They presented a case study where, based on data from multiple spacecraft and high-frequency radars, it was proposed that the apparent continuous arc actually consisted of two parts. Unlike other previous models, they proposed that two different mechanisms are responsible for the theta aurora formation at dayside and nightside

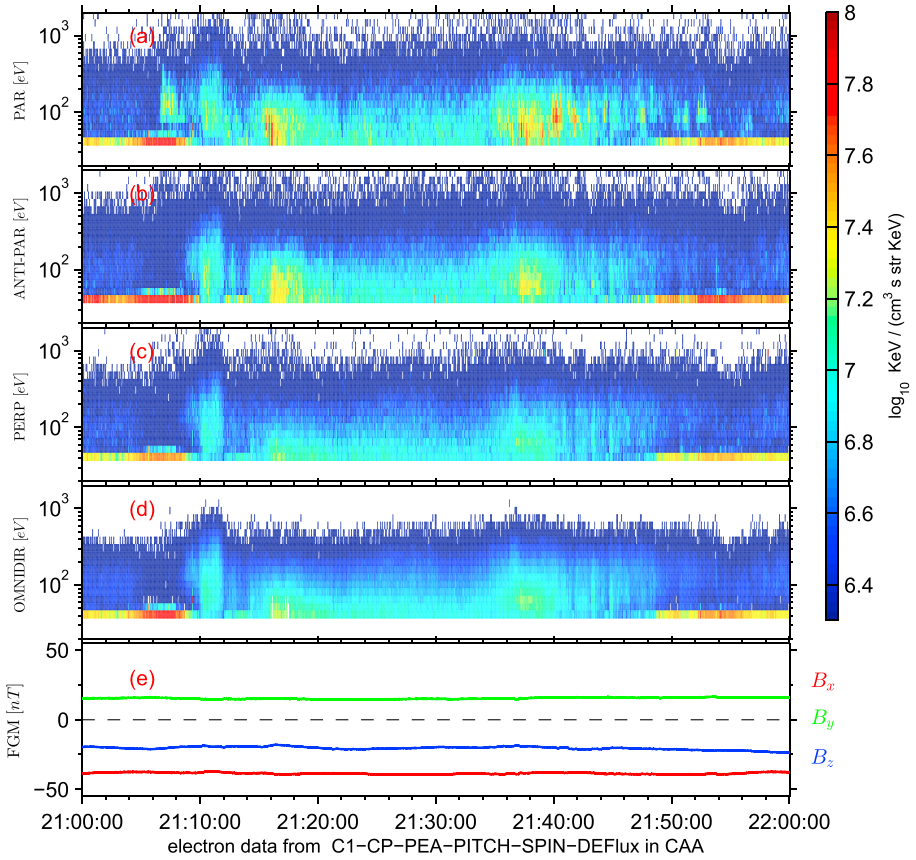

Figure 5. (a–e) Differential energy flux of electron and magnetic field measured by Cluster on 27 September 2004. From top to bottom, parallel, antiparallel, perpendicular to the magnetic field, and omnidirectional electron fluxes along with magnetic field measurements are presented.

regions. According to *Eriksson et al.* [2005], high-latitude lobe reconnection is necessary to generate the dayside part of the transpolar arc. At the nightside region, upward field aligned currents of the Harang discontinuity create the nightside part of the arc. There exist several other observations showing different flow directions on the same transpolar arc, which strengthens the idea suggested by *Eriksson et al.*'s [2005] [e.g., *Liou et al.*, 2005; *Nielsen et al.*, 1990]. The observations of the electron precipitation at the dayside and nightside parts [*Park et al.*, 2012] also point to the difference between these regions. For the event of 27 September 2004 event, the GUVI high-resolution data also show some fine structure of the transpolar arc. This also can be in favor of the Eriksson's model, since the lower spatial resolution of IMAGE WIC would show the more complex structure of the theta aurora as a one continuous entity. But for the formation of the nightside part of the arc, from our observations in this event, we cannot distinguish whether it is caused by Harang discontinuity as suggested by *Eriksson et al.* [2005] or magnetotail reconnection by *Milan et al.* [2005].

Fear et al. [2014] reported the presence of a double loss cone within high-latitude, high-altitude plasma signatures with higher energy than those observed by *Shi et al.* [2013], indicative of the signatures being observed on closed magnetic field lines. However, the examination of the pitch angle distribution of the entry plasma electrons (shown in Figure 1c) for the 27 September 2004 event did not reveal the existence of double loss cones. This is shown in Figure 5. In that Figure, the parallel, antiparallel, and perpendicular to magnetic field electron distributions are shown, along with Cluster FGM measurements. Figure 5 shows that the electron flux is not dominating in the perpendicular direction. The observation of double loss cones similar to those reported in *Fear et al.* [2014] would be a very strong evidence of the closed field line configuration. A bidirectional distribution of the electrons observed for this event as it can be seen from Figure 5. The enhanced fluxes in parallel to magnetic field direction near 21:16 and 21:40 indicate the

presence of electron upflows. Since the event occurred at the southern hemisphere, these dominating in the parallel to the field electrons move toward the direction opposite to the Earth.

Double loss cones are a sufficient but not necessary condition for the closed field line condition. In the event discussed in this paper, we did not find fluxes peaking at the perpendicular direction. The absence of the loss cone does not mean automatically an open field line configuration. Therefore, the topology of the field lines in this example cannot be convincingly determined from the data in this example. In *Shi et al.*'s [2013] mechanism, the present observations would be interpreted as plasma of solar wind origin which has entered on open magnetic field lines, whereas in *Fear et al.*'s [2014] interpretation, the plasma would be explained as being on the outer edge of a closed field line region where a double loss cone has not yet formed (as observed in Figure 3a of *Fear et al.* [2014], either side of the double loss cone, although we note again the difference in energy between the plasma observations in the two studies).

Further analysis of similar events would be necessary to improve the understanding of the role of solar wind entry at high latitudes for the formation and evolution of transpolar arcs.

Acknowledgments

We thank FGM, CIS teams for providing the Cluster data, the DMSP plasma instrument team, WIC, and GUVI teams for the IMAGE and TIMED data. The OMNI data were obtained from the GSFC/SPDF OMNIWeb interface at http://omniweb.gsfc.nasa.gov. We are grateful to graduate students Xiaochen Shen and Shutao Yao for the help during the preparation of the manuscript. This work is supported by grants NNSFC 41322031, 41031065, and 41404131; China Postdoctoral Science Foundation grant 2014M561914; by the Specialized Research Fund for State Key Laboratories, Ministry of Education of China (NCET-12-0332); and Shandong Natural Science Foundation (grant JQ201112). B.M. thanks China International Postdoctoral Exchange Program.

Larry Kepko thanks the reviewers for their assistance in evaluating this paper.

References

Baker, J. B., R. A. Greenwald, J. M. Ruohoniemi, K. Oksavik, J. W. Gjerloev, L. J. Paxton, and M. R. Hairston (2007), Observations of ionospheric convection from the Wallops SuperDARN radar at middle latitudes, *J. Geophys. Res.*, *112*, A01303, doi:10.1029/2006JA011982.

Balogh, A., et al. (2001), The Cluster magnetic field investigation: Overview of in-flight performance and initial results, *Ann. Geophys.*, *19*, 1207–1217, doi:10.5194/angeo-19-1207-2001.

Chang, S.-W., et al. (1998), A comparison of a model for the theta aurora with observations from Polar, Wind, and SuperDARN, *J. Geophys. Res.*, *103*(A8), 17,367–17,390, doi:10.1029/97JA02255.

Chiu, Y. T., N. U. Crooker, and D. J. Gorney (1985), Model of oval and polar cap arc configurations, *J. Geophys. Res.*, *90*(A6), 5153–5157, doi:10.1029/JA090iA06p05153.

Craven, J. D., J. S. Murphree, L. A. Frank, and L. L. Cogger (1991), Simultaneous optical observations of transpolar arcs in the two polar caps, *Geophys. Res. Letters*, *18*, 2297, doi:10.1029/91GL02308.

Elphinstone, R. D., et al. (1995), The double oval UV auroral distribution: 1. Implications for the mapping of auroral arcs, *J. Geophys. Res.*, *100*(A7), 12,075–12,092, doi:10.1029/95JA00326.

Erickson, G. M., R. W. Spiro, and R. A. Wolf (1991), The physics of the Harang discontinuity, *J. Geophys. Res.*, *96*(A2), 1633–1645, doi:10.1029/90JA0234.

Eriksson, S., et al. (2005), On the generation of enhanced sunward convection and transpolar aurora in the high-latitude ionosphere by magnetic merging, *J. Geophys. Res.*, *110*(A11), A11218, doi:10.1029/2005JA011149.

Fear, R. C., and S. E. Milan (2012a), The IMF dependence of the local time of transpolar arcs: Implications for formation mechanism, *J. Geophys. Res.*, *117*(A3), A03213, doi:10.1029/2011JA017209.

Fear, R. C., and S. E. Milan (2012b), Ionospheric flows relating to transpolar arc formation, *J. Geophys. Res.*, *117*, A09230, doi:10.1029/2012JA017830.

Fear, R. C., S. E. Milan, R. Maggiolo, A. N. Fazakerley, I. Dandouras, and S. B. Mende (2014), Direct observation of closed magnetic flux trapped in the high-latitude magnetosphere, *Science*, *346*, 1506–1510, doi:10.1126/science.1257377.

Frank, L. A., J. D. Craven, J. L. Burch, and J. D. Winningham (1982), Polar views of the Earth's aurora with dynamics explorer, *Geophys. Res. Lett.*, *9*, 1001–1004, doi:10.1029/GL009i009p01001.

Frank, L. A., et al. (1986), The theta aurora, *J. Geophys. Res.*, *91*, 3177, doi:10.1029/JA091iA03p03177.

Goudarzi, A., et al. (2008), Multi-instrumentation observations of a transpolar arc in the northern hemisphere, *Ann. Geophys.*, *26*(1), 201–210.

Gussenhoven, M. S., and E. G. Mullen (1989), Simultaneous relativistic electron and auroral particle access to the polar caps during interplanetary magnetic field B_z northward: A scenario for an open field line source of auroral particles, *J. Geophys. Res.*, *94*(A12), 17,121–17,132, doi:10.1029/JA094iA12p17121.

Hardy, D. A., E. G. Holeman, W. J. Burke, L. C. Gentile, and K. H. Bounar (2008), Probability distributions of electron precipitation at high magnetic latitudes, *J. Geophys. Res.*, *113* A06305, doi:10.1029/2007JA012746.

Huang, C. Y., J. D. Craven, and L. A. Frank (1989), Simultaneous observations of a theta aurora and associated magnetotail plasmas, *J. Geophys. Res.*, *94*(A8), 10,137–10,143, doi:10.1029/JA094iA08p10137.

Iijima, T., T. A. Potemra, L. J. Zanetti, and P. F. Bythrow (1984), Large-scale Birkeland currents in the dayside polar region during strongly northward IMF: A new Birkeland current system, *J. Geophys. Res.*, *89*(A9), 7441–7452, doi:10.1029/JA089iA09p07441.

King, J. H., and N. E. Papitashvili (2005), Solar wind spatial scales in and comparisons of hourly Wind and ACE plasma and magnetic field data, *J. Geophys. Res.*, *110*, A02104, doi:10.1029/2004JA010649.

Koustov, A., K. Hosokawa, N. Nishitani, T. Ogawa, and K. Shiokawa (2008), Rankin Inlet PolarDARN radar observations of duskward moving Sun-aligned optical forms, *Ann. Geophys.*, *26*, 2711–2723, doi:10.5194/angeo-26-2711-2008.

Koustov, A., K. Hosokawa, N. Nishitani, K. Shiokawa, and H. Liu (2012), Signatures of moving polar cap arcs in the *F*-region PolarDARN echoes, *Ann. Geophys.*, *30*, 441–455, doi:10.5194/angeo-30-441-2012.

Kozlovsky, A., A. Aikio, T. Turunen, H. Nilsson, T. Sergienko, V. Safargaleev, and K. Kauristie (2007), Dynamics and electric currents of morningside Sun-aligned auroral arcs, *J. Geophys. Res.*, *112*, A06306, doi:10.1029/2006JA012244.

Kullen, A. (2000), The connection between transpolar arcs and magnetotail rotation, *Geophys. Res. Lett.*, *27*, 73–76, doi:10.1029/1999GL010675.

Kullen, A. (2012), Transpolar arcs: Summary and recent results, in *Auroral Phenomenology and Magnetospheric Processes: Earth and Other Planets*, *Geophys. Monogr. Ser.*, vol. 197, edited by A. Keiling et al., pp. 69–80, AGU, Washington, D. C., doi:10.1029/2011GM001183.

Kullen, A., and P. Janhunen (2004), Relation of polar auroral arcs to magnetotail twisting and IMF rotation: A systematic MHD simulation study, *Ann. Geophys.*, *22*, 951–970, doi:10.5194/angeo-22-951-2004.

Kullen, A., M. Brittnacher, J. A. Cumnicllk, and L. G. Blomberg (2002), Solar wind dependence of the occurrence and motion of polar auroral arcs: A statistical study, *J. Geophys. Res.*, *107*(A11), 1362, doi:10.1029/2002JA009245.

Liou, K., J. M. Ruohoniemi, P. T. Newell, R. Greenwald, C. I. Meng, and M. R. Hairston (2005), Observations of ionospheric plasma flows within theta auroras, *J. Geophys. Res.*, *110*, A03303, doi:10.1029/2004JA010735.

Lyons, L. R. (1985), A simple model for polar cap convection patterns and generation of θ auroras, *J. Geophys. Res.*, *90*(A2), 1561–1567, doi:10.1029/JA090iA02p01561.

Maggiolo, R., M. Echim, J. De Keyser, D. Fontaine, C. Jacquey, and I. Dandouras (2011), Polar cap ion beams during periods of northward IMF: Cluster statistical results, *Ann. Geophys.*, *29*, 771–787, doi:10.5194/angeo-29-771-2011.

Mailyan, B., C. Munteanu, and S. Haaland (2008), What is the best method to calculate the solar wind propagation delay?, *Ann. Geophys.*, *26*, 2383–2394, doi:10.5194/angeo-26-2383-2008.

Makita, K., C.-I. Meng, and S.-I. Akasofu (1991), Transpolar auroras, their particle precipitation, and IMF B_y component, *J. Geophys. Res.*, *96*(A8), 14,085–14,095, doi:10.1029/90JA02323.

Mawson, D. (1916), Auroral observations at the Cape Roys Station, British Antarctic Expedition 1908, *Trans. R. Soc. S. Australia*, *40*, 151–212.

McComas, D. J., S. J. Bame, P. Barker, W. C. Feldman, J. L. Phillips, P. Riley, and J. W. Griffee (1998), Solar Wind Electron Proton Alpha Monitor (SWEPAM) for the Advanced Composition Explorer, *Space Sci. Rev.*, *86*, 563.

Mende, S. B., et al. (2000), Far ultraviolet imaging from the IMAGE spacecraft: 3. Spectral imaging of Lyman-α and OI 135.6 nm, in *The Image Mission*, pp. 287–318, Springer, Netherlands, doi:10.1023/A:1005292301251.

Milan, S. E., B. Hubert, and A. Grocott (2005), Formation and motion of a transpolar arc in response to dayside and nightside reconnection, *J. Geophys. Res.*, *110*, A01212, doi:10.1029/2004JA010835.

Naehr, S. M., and F. R. Toffoletto (2004), Quantitative modeling of the magnetic field configuration associated with the theta aurora, *J. Geophys. Res.*, *109*, A07202, doi:10.1029/2003JA010191.

Newell, P. T., and C.-I. Meng (1995), Creation of theta-auroras: The isolation of plasma sheet fragments in the polar cap, *Science*, *270*(5240), 1338–1341, doi:10.1126/science.270.5240.1338.

Nielsen, E., J. D. Craven, L. A. Frank, and R. A. Heelis (1990), Ionospheric flows associated with a transpolar arc, *J. Geophys. Res.*, *95*(A12), 21,169–21,178, doi:10.1029/JA095iA12p21169.

Ostgaard, N., S. B. Mende, H. U. Frey, L. A. Frank, and J. B. Sigwarth (2003), Observations of non-conjugate theta aurora, *Geophys. Res. Lett.*, *30*(21), 2125, doi:10.1029/2003GL017914.

Park, J., et al. (2012), Dayside and nightside segments of a polar arc: The particle characteristics, *J. Geophys. Res.*, *117*, A07224, doi:10.1029/2011JA017323.

Paxton, L. J., et al. (2004), GUVI: A hyperspectral imager for geospace, in *Instruments, Science, and Methods for Geospace and Planetary Remote Sensing*, Proc. SPIE 5660, vol. 228, edited by C. A. Nardell et al., pp. 227–240, The International Society for Optical Engineering, Bellingham, Wash, doi:10.1117/12.579171.

Reiff, P. H., and J. L. Burch (1985), IMF B_y-dependent plasma flow and Birkeland currents in the dayside magnetosphere: 2. A global model for northward and southward IMF, *J. Geophys. Res.*, *90*(A2), 1595–1609, doi:10.1029/JA090iA02p01595.

Reme, H., et al. (2001), First multispacecraft ion measurements in and near the Earth's magnetosphere with the identical Cluster ion spectrometry (CIS) experiment, *Ann. Geophys.*, *19*, 1303–1354, doi:10.5194/angeo-19-1303-2001.

Rezhenov, B. V. (1995), A possible mechanism for θ aurora formation, *Ann. Geophys.*, *13*, 698–703, doi:10.1007/s00585-995-0698-3.

Shi, Q. Q., et al. (2013), Solar wind entry into the high-latitude terrestrial magnetosphere during geomagnetically quiet times, *Nat. Commun.*, *4*, 1466, doi:10.1038/ncomms2476.

Shiokawa, K., T. Ogino, K. Hayashi, and D. J. McEwen (1997), Quasiperiodic poleward motions of morningside Sun-aligned arcs: A multievent study, *J. Geophys. Res.*, *102*, 24,325–24,332, doi:10.1029/97JA02383.

Slinker, S. P., J. A. Fedder, J. M. Ruohoniemi, and J. G. Lyon (2001), Global MHD simulation of the magnetosphere for November 24, 1996, *J. Geophys. Res.*, *106*(A1), 361–380, doi:10.1029/2000JA000603.

Smith, C. W., J. L'Heureux, N. F. Ness, M. H. Acuna, L. F. Burlaga, and J. Scheifele (1998), The ACE magnetic fields experiment, *Space Sci. Rev.*, *86*, 613–632, doi:10.1023/A:1005092216668.

Sojka, J. J., L. Zhu, D. J. Crain, and R. W. Schunk (1994), Effect of high-latitude ionospheric convection on Sun-aligned polar caps, *J. Geophys. Res.*, *99*, 8851–8863, doi:10.1029/93JA02667.

Valladares, C. E., H. C. Carlson, and K. Fukui (1994), Interplanetary magnetic field dependency of stable Sun-aligned polar cap arcs, *J. Geophys. Res.*, *99*(A4), 6247–6272, doi:10.1029/93JA03255.

Vasyliunas, V. M. (1970), Mathematical models of magnetospheric convection and its coupling to the ionosphere, in *Particles and Fields in the Magnetosphere*, edited by B. M. McCormac, pp. 60–71, Springer, Dordrecht, Netherlands, doi:10.1007/978-94-010-3284-1_6.

Zhu, L., R. W. Schunk, and J. J. Sojka (1997), Polar cap arcs: A review, *J. Atmos. Sol. Terr. Phys.*, *59*, 1087–1126, doi:10.1016/S1364-6826(96)00113-7.